



CHARACTERIZATION OF *MUSANGA CECROPIOIDES* LEAF AS ECO-FRIENDLY INHIBITOR FOR PROTECTION OF OIL AND GAS EQUIPMENT IN ACIDIC ENVIRONMENT

Munir Zubair SIRAJO,^a Idawu Yakubu SULEIMAN,^{b,c,d,*} Kabiru MU'AZU,^e Njoku Romanus EGWUONWU,^b Adams Sani MUHAMMAD,^b Ogheneme Ogheneborhie CLIFFORD,^f Raheem Rasheed ADEBAYO,^b Omoraka AUSTIN,^f Amhenrior Ernest OSARHEKPAMHEN,^f Ijeamiran Tunde MARVELOUS^f and Akponah OTARIGHO^f

^aPetroleum Technology Development Fund, Abuja, F. C. T., Nigeria

^bDepartment of Metallurgical and Materials Engineering, University of Nigeria, Nsukka, Nigeria

^cAfrican Centre of Excellence for Sustainable Power and Energy Development (ACE-SPED) University of Nigeria, Nsukka

^dDepartment of Metallurgical and Materials Engineering, Federal University Lokoja, Nigeria

^eDepartment of Pilot Plant and Fabrication, National Research Institute for Chemical Technology Zaria, Nigeria

^fDepartment of Mechanical Engineering, Federal Polytechnic Orogun, Delta State, Nigeria

Received February 3, 2025

In the continuation of the possibility of using green corrosion inhibitors as sustainability in corrosion mitigation for oil and gas applications, *Musanga cereoipoides* (MC) leaf extract as a corrosion inhibitor for steel pipeline in 0.5 M sulphuric acid using both gravimetric and potentiodynamic polarization techniques was investigated. The leaves were characterized by both quantitative, and qualitative analyses, and Fourier Transform Infrared (FT-IR). Characterization of the substrates before and after corrosion tests were investigated by scanning electron microscope equipped with energy-dispersive X-ray spectroscopy. The inhibitor concentration, time and temperature were varied in the range of 3–15 g/l, 2–14 days and 30–60°C at intervals of 3 g/l, 2 days, and 10°C intervals respectively. The corrosion rate increased with the increasing temperature and decreased with increases in inhibitor concentrations and time, respectively. Maximum inhibition efficiency of 95.80% occurred at the optimal value of 12 g/l of the inhibitor concentration. The results revealed phytoconstituents such as tannins, alkaloids, saponins, and flavonoids. The FT-IR results indicated the following functional/elements present as N=C=S, C-Br, OH, NH, C-N, C-Cl, P-O-C, C-O etc which were responsible for the protection of steel pipelines in an acidic environment. The coupons without green inhibitor were rough, and severe pits and cracks occurred, while the surface of the steel pipeline with green inhibitor was smooth. The molecules of the green inhibitor were absorbed on the adsorbate's surface. The potentiodynamic polarization results showed that the green inhibitor acted as a mixed-type inhibitor. The green inhibitor served as an alternative to synthetic inhibitors. The values of inhibition efficiency obtained are well above the minimum acceptable limit of 70% required of a good inhibitor. It can therefore be used in the formulation of paints.



* Corresponding author: idawu.suleiman@unn.edu.ng

INTRODUCTION

Steel pipelines are critical components in various industrial applications, including the transportation of crude oil, gas, and chemicals. However, their exposure to acidic environments, particularly during operations involving acidic cleaning or enhanced oil recovery, makes them highly susceptible to corrosion. Corrosion not only compromises the structural integrity of pipelines but also leads to significant economic losses and environmental hazards.¹

Inorganic inhibitors such as chromates, phosphates, nitrates and organic inhibitors having heteroatoms and/or π -bonds compounds are the most commonly used metal corrosion inhibitors. The inorganic compounds have been observed to oxidize metal surfaces by forming impervious films that deny aggressive agents in the environment access to the surface.² However, inorganic inhibitors are very expensive and not degradable and their disposals create pollution problems which make them harmful to the environment.³

The search for effective, eco-friendly corrosion inhibitors has garnered considerable attention as industries shift towards sustainable practices. Plant-based inhibitors, derived from renewable and biodegradable natural sources, have emerged as promising alternatives to conventional chemical inhibitors.⁴ The adsorption ability and efficiency of the inhibitors are based on their chemical composition, molecular structure, type of functional groups, and their attraction towards the coupon surface. Recently, research has been investigated and published on using natural inhibitors such as plant extracts to inhibit the corrosion of steel pipelines in different environments.⁵

Previous work suggested that the adsorption of an inhibitor on a metal surface depends on the nature, surface charge of the metal, adsorption mode, its chemical structure and the type of the electrolyte solution.⁶ The relationship between adsorption and corrosion inhibition is important in that corrosion inhibition is a surface process and the degree of protection of metal is a function of adsorption.⁷ Another work carried out by⁸ also agreed that organic compounds containing hetero-

atoms such as phosphorus (P), nitrogen (N), sulphur (S), and oxygen (O) with high electron density as well as those containing multiple bonds are effective corrosion inhibitors. All plant products are organic; their constituents are tannins, organic and amino acids, saponins, alkaloids, flavonoids, glycosides and pigments are known to exhibit inhibiting action.⁹⁻¹⁷

Oil and gas equipment corrosion, particularly in sulphuric acidic environments, remains a critical challenge for the industry. Acidic conditions are prevalent in processes such as acidizing, descaling, and enhanced oil recovery, leading to accelerated degradation of metallic surfaces. This not only jeopardizes the structural integrity and operational efficiency of equipment but also incurs substantial economic and environmental costs.

This work is designed to carry out the possibility of using *Musanga cecropioides* (MC) a non-toxic plant as a corrosion inhibitor for steel pipelines in 0.5 M H₂SO₄ solution. The surface morphology of the coupons was characterized using Scanning Electron Microscopy with energy dispersive spectroscopy (SEM/EDS) to study the corrosion before and after the tests. The plant extract was also characterized by quantitative and qualitative analyses, and Fourier Transform Infrared Spectroscopy (FT-IR). By combining experimental results, the study aims to elucidate the mechanism of inhibition, assess the practical viability of the extract, and contribute to the development of sustainable corrosion mitigation strategies.

MATERIALS AND METHODS

Materials preparation

The steel pipeline used for this study was obtained from Ajaokuta Steel Company (ASC) in Kogi, State, Nigeria. The chemical composition of the steel pipeline used for both weight loss and potentiodynamic polarization was determined by X-ray fluorescence (XRF) and is presented in Table 1.

Table 1

Chemical composition of steel pipeline

Element	Fe	C	Si	Mn	P	S	Co	Mo	Ni	Al	Cu
% Wi.	99.01	0.169	0.033	0.434	0.016	0.014	0.05	0.014	0.18	0.002	0.015

Preparation of inhibitor

Fresh leaves of *Musanga cecropioides* (MC) leaves presented in Fig. 1 below were obtained from the university farm land, Nsukka Nigeria. Cleaning, and drying of the leaves at room temperature for three days were carried out. Dried leaves were then ground into fine powder using a mortar and pestle. About five hundred grams (500 gm) of ground

sample was then extracted in 1.5 L of 70% ethanol and 30% distilled water was used as solvent using the maceration method by separating funnel. The extract and the final stage of collecting the liquid at 110°C before evaporation was used. The concentration of the stock solution was expressed in terms of gram per litre (g/L) and the concentration of 3–15 g/L of the extract was prepared according to the work of.^{18,19}



Fig. 1 – *Musanga cecropioides* leaves.

Solution Preparation

Solutions of 0.5 M H₂SO₄ were prepared by diluting of analytical grade with double distilled water. Extracts were dissolved in the acid solution at the required concentrations (g/L). The solution in the absence of an inhibitor was taken as blank (0) for comparison purposes.¹⁹ The test solutions were freshly prepared before each experiment by adding *Musanga cecropioides* leaves (MC) extract directly to the corrosive solution. Concentrations of *Musanga cecropioides* leaf extract used were: 0, 3, 6, 9, 12, and 15 g/L respectively. Experiments were performed in triplicate to ensure good results.

Determination of Phytoconstituents of the Leaf Extract

The phytochemical constituents of the leaf were determined by both quantitative and qualitative methods. The analyses were carried out at the Multi-Users Laboratory, Ahmadu Bello University Zaria, Nigeria. The results are presented in both Tables 2 and 3 respectively.

Preparation of Specimens

Steel pipelines were mechanically cut into cylindrical shapes of 10 mm by 8 mm with the following chemical compositions shown in Table 1. The specimens were polished mechanically with emery papers of 400–1600 grades and subsequently decreased and stored in the desiccators to avoid re-oxidation. The weight of the samples was taken before and after the weight loss carried out by.²⁰

Weight Loss Measurements

The previously polished and degreased specimens of size 10 mm by 8 mm coupons were used for weight loss studies. Already-weighted specimens were separately immersed in 500 millilitres (ml) of 0.5 M H₂SO₄ solutions containing 0, 3, 6, 9, 12, and 15 g/L of MC extract for 2, 4, 6, 8, 10, 12 and 14 days respectively. After the elapsed time, the specimens were taken out, washed, dried and reweighed. All the experiments were performed in triplicate, and average values were recorded. The experiment was carried out at different temperatures

of 30, 40, 50 and 60°C respectively. From the measured weight loss data, the corrosion rate (mpy) and the inhibition efficiency (IE) were calculated using Eqs. 1–3 below as reported by.^{21–23}

$$\text{Corrosion rate (mpy)} = \frac{534W}{DAT} \quad (1)$$

where W, D, A and T will be in units of milligrams, grams per cubic centimetre, square inches and hours, respectively. The inhibition efficiency (IE %) and surface coverage (θ) were calculated from the following equations:

$$\text{Inhibition efficiency (IE \%)} = \frac{CR_a}{CR_p} \times \frac{100}{1} \quad (2)$$

$$\text{Surface coverage } (\theta) = \frac{CR_a - CR_p}{CR_a} \quad (3)$$

where CR_a and CR_p are the corrosion rates in the absence and the presence of the extract, respectively.

Electrochemical Measurements

Potentiodynamic polarization technique

The electrochemical measurements were performed in a conventional three-electrode assembly containing a cylindrical carbon steel specimen with an exposed area of 1 cm² as working

electrode (WE), a platinum foil of surface area 2 cm² as counter electrode and a saturated calomel electrode (SCE) provided with a Luggin capillary as a reference electrode. They were immersed in 0.5 M H₂SO₄ solution until a steady-state open-circuit potential (OCP) was obtained. Potentiodynamic polarization measurements were done using an Autolab potentiostat (PGSTAT30 computer-controlled) with the General-Purpose Electrochemical Software (GPES) package version 4.9. The H₂SO₄ solution was degassed with ultrapure nitrogen bubbling to avoid any reactions with dissolved oxygen. Tafel polarization measurements were made for a potential range of –200 mV to 7200 mV concerning OCP at a scan rate of 1 mV/s. From the electrochemical studies, corrosion potential and corrosion current were calculated. All the tests were performed at a temperature of 30°C. The inhibitor efficiency was then calculated from Equation 4 as given by.^{24,25}

$$IE \% = \frac{i_{corr} - i'_{corr}}{i_{corr}} \times 100\% \quad (4)$$

where i_{corr} and i'_{corr} are the corrosion current densities of steel pipeline in the absence and presence of the inhibitor respectively. The parameters used for this method are presented in Table 4.

Table 4

Parameters used in the potentiodynamic electrochemical technique at 35 °C

Parameters	Material
Initial voltage (V) Wrt OCP	–1.5
Final voltage (V) Wrt OCP	1.5
Scan rate (mV/s)	0.01

Characterization of *Musanga cecropioides* leaves extract by FT-IR Spectroscopy

A small quantity of *Musanga cecropioides* powdered sample was then exposed to infrared radiation. The sample molecules selectively absorb radiation of a specific wavelength which causes the change of dipole moment of the sample molecules.²⁶ The commonly used region for infrared absorption spectroscopy was from 3500 to 500 cm^{–1}. This is because the absorption radiation is within the region. The FT-IR was carried out using the Perkin Elmer 2000 Model at the Energy Centre, University of Nigeria, Nsukka. The spectra obtained were then interpreted using Standard Library.²⁷

Characterization of the coupons

Scanning Electron Microscope (SEM) was used to provide basic information about the microstructure of the coupons. The samples were cut from the control. The cut samples were mechanically ground progressively on grades of SiC-impregnated emery paper (80–600 grits). The coupons were selected for SEM after the electrochemical analyses. The microstructure and the chemical compositions of the phases present in the test samples were studied. The SEM was operated at an accelerating voltage of 5 to 20 kV.

RESULTS AND DISCUSSION

Phytoconstituents of the *Musanga cecropioides* (MC) extract

The detailed results of phytochemical constituents carried out on the extract by both quantitative and qualitative analyses showed that *Musanga cecropioides* (MC) contains Saponins, Tannins, Alkaloids, Flavonoids, Glycosides and

Volatile oil. Tables 2 and 3 presented the quantitative and qualitative analyses of *Musanga cecropioides* (MC) extract respectively. The results show that the constituents can be adsorbed onto the metallic surface by blocking the active corrosion site or reducing the evolution of hydrogen gas at the cathode. This may be attributed to the fact that some of these phytoconstituents contain heteroatoms such as O, N, S, P, and both aromatic and functional groups and also agree with the findings of.²⁸

Table 2

The qualitative analysis of *Musanga cecropioides* (MC) leaf extract

<i>Musanga cecropioides</i> (MC) leaf extract	Tannins	Saponins	Flavonoids	Glycosides	Alkaloids	Volatile oil
	+	+	-	+	+	+

Table 3

The quantitative analysis of *Musanga cecropioides* (MC) leaf extract

<i>Euphoba Hirtal</i> (EH) leaf	Tannins (%)	Saponins (%)	Flavonoids (%)	Glycosides (%)	Alkaloids (%)	Volatile oil (%)
	15.10±0.01	3.23±0.03	0.000	0.65±0.12	1.34±0.03	0.65±0.24

Fourier Transforms Infrared (FT-IR) Spectroscopy results

Figures 2 and 3 show the IR absorption spectra and their functional groups. The prominent peaks obtained from the FT-IR spectroscopy for the *Musanga cecropioides* (MC) extract were presented in Table 5 and confirmed in the previous works.^{18,28}

The inhibitor showed an effective anticorrosion potential and the results indicated that the inhibition mechanism involved blockage of the steel pipeline by inhibitor molecules via adsorption. In general, the phenomenon of adsorption was influenced by the nature and surface charge of the metal, the type of aggressive electrolyte, and the chemical structure of inhibitors.²⁸

6:43:14 AM 4/11/2024

MODEL: IR AFFINITY-1

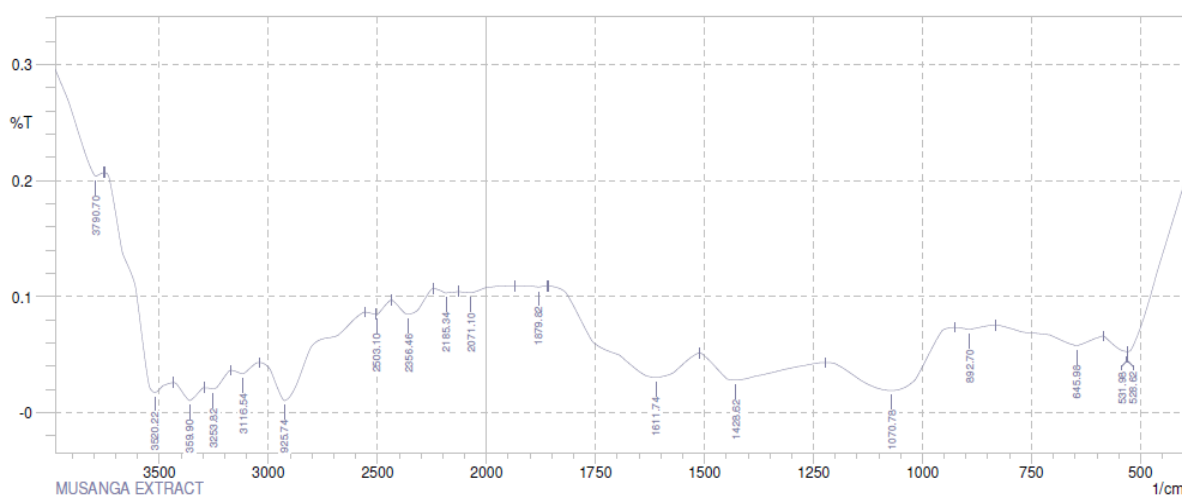


Fig. 2 – FT-IR transmittance spectra of *Musanga cereipoides* (MC).

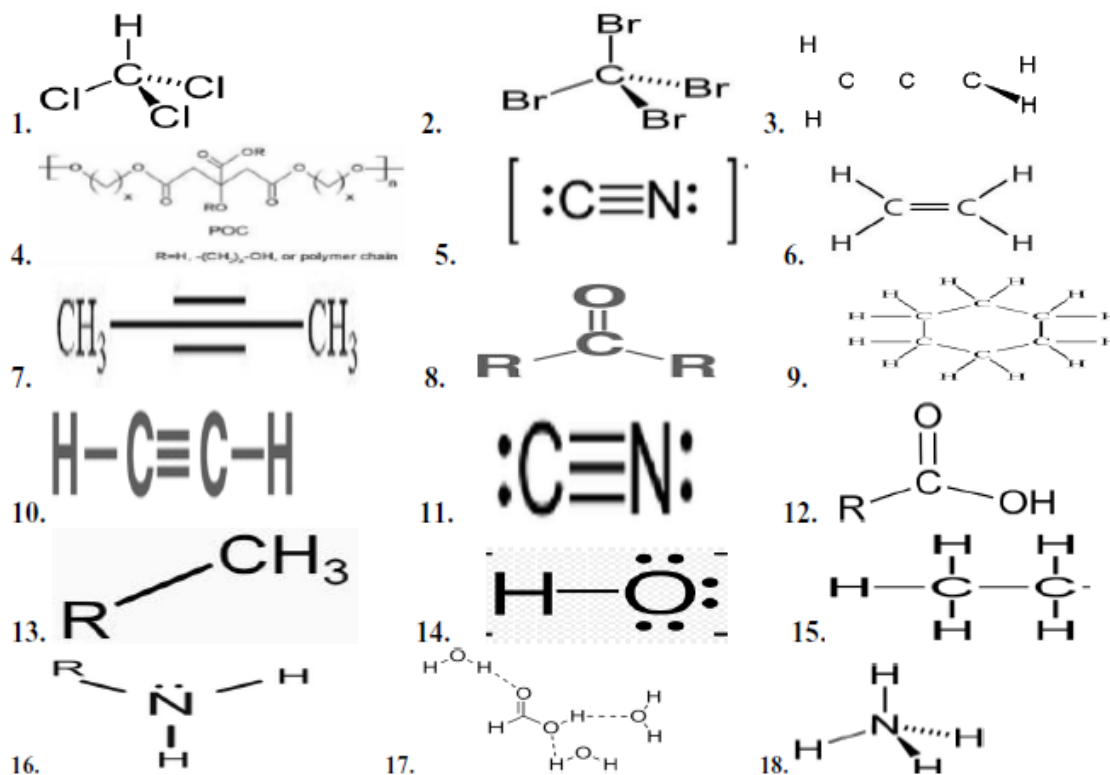


Fig. 3 – FT-IR showing the functional groups/structures present in *Musanga cecropioides* (MC).

Table 5

Prominent peaks obtained from reflectance FTIR spectroscopy for MC extract

S/No	Frequency (cm ⁻¹)	Band assignment
1.	528.62	Chlorocompound, (C-Cl)
2.	531.98	C- Br, OH, NH,
3.	645.98	C-CH ₂ - CH ₂ -Br
4.	892.7	P-O-C stretch (Aromatic phosphates)
5.	1070.78	C-N stretching (Amine)
6.	1428.62	CH ₂
7.	1611.74	C=C stretching (α,β-unsaturated ketone)
8.	1879.82	C=O stretching
9.	2071.1	C-H deformation
10.	2185.34	C=C Stretching bond of alkynes molecule
11.	2356.46	C-N
12.	2503.1	Carboxyl acid
13.	2925.74	Methyl group
14.	3116.54	O-H (H-bonded)
15.	3253.82	O-H stretch, Hydroxyl group, H-bonded
16.	3359.9	N-H (2°-amines)
17.	3520.22	O-H (H-bonded)
18.	3790.7	NH and C=O

Visual observations of the corroded surfaces

Visual observations of the two categories of coupons (inhibited and uninhibited) revealed that the coupons changed from bright and shining surfaces to dull and brownish surfaces with time. The solution of the acid turned dark brown, with macro cracks on the surfaces observed on the coupons, indicating a severe corrosion attack by the acid. Also, pit formations were seen on the coupons, which indicated a localized corrosion attack by the acid medium. The pit attack is more severe on a sample without *Musanga cecropioides* extract.

Effect of *Musanga cecropioides* extract on steel pipelines

Weight loss measurements were performed on steel pipelines immersed in 0.5 M H₂SO₄ solutions with and without (MC) extract for seven (14) days. The results obtained in the absence and the presence of the inhibitor at various concentrations are presented in Fig. 4. It can be seen that inhibition efficiency increases with the increase in inhibitor concentrations, which could be due to the increase

in the mass and charge transfer to the steel pipeline surface leading to the adsorption of inhibitor molecules and reduction in the metal dissolution as shown in the leaves characterizations by FT-IR. Further increase in the inhibitor concentration causes little or negligible change and the highest inhibition efficiency occurred at the optimum concentration of the inhibitor (12 g/l). Owing to the acidity of the corrosive medium, the extract which contains the phytochemical constituents, and functional groups from the FT-IR could not remain in the solution in its free base state and may exist as a neutral species or in its cationic form which was presented in table 4 respectively. This assertion also agrees with the findings of the previous studies.²⁹ The high inhibition efficiency recorded could be possibly because SO₄²⁻ was hydrated in H₂SO₄ and this can be poorly adsorbed onto the metal surface leaving more active sites for the adsorption of the inhibitor–neutral species – and thus inhibition efficiency increased with an increase in concentrations of the inhibitor in H₂SO₄ medium. Hence, it can be concluded that while adding the inhibitor to the H₂SO₄ solution anions like C-N, NH, C=O, and OH are present in the inhibitor solution, and the unshared pair of electrons is present.³⁰

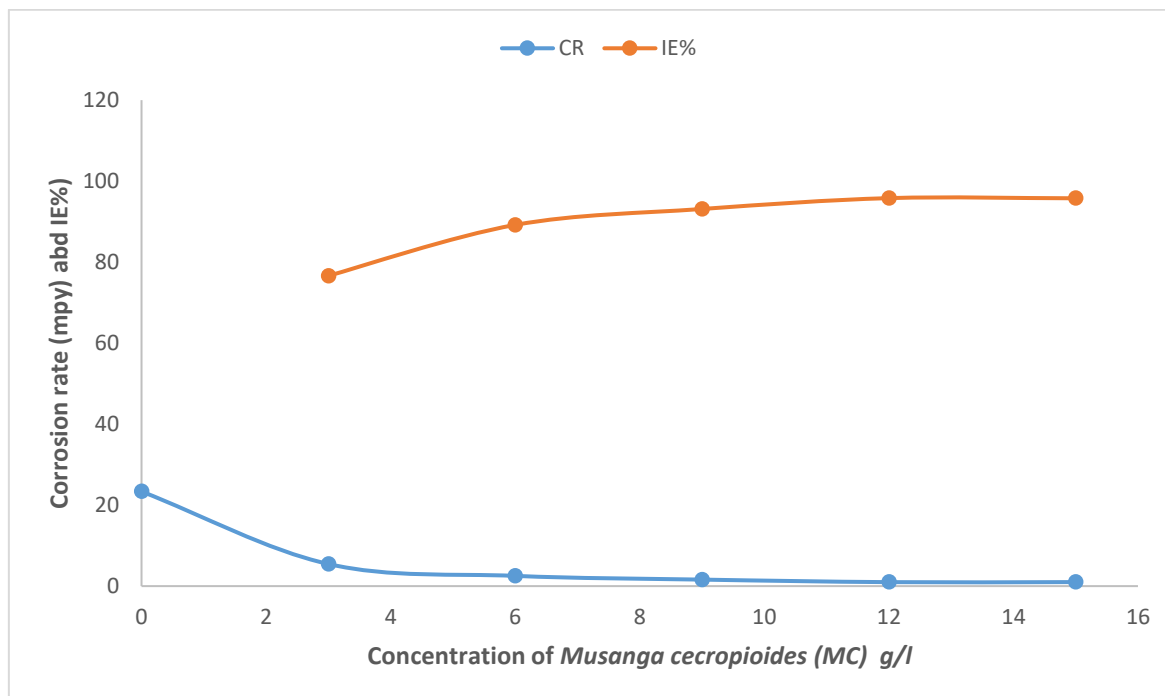


Fig. 4 – Variation of Corrosion rate (mpy) and inhibition efficiency (% IE) with inhibitor concentration at 308 K.

Effect of Temperature on Inhibition Efficiency

The temperature effect on the inhibition efficiency investigated on mild steel at a range of

30– 60 °C is shown in Fig. 5. The inhibition efficiency decreases with an increase in temperature. At higher temperatures, the hydrogen evolution increases on the metal surface and leads

to desorption of the adsorbed inhibitor film from the metal surface as noted. It could also be attributed to

an increase in the rates of ionization and diffusion of active species in the corrosion Process.^{31,32}

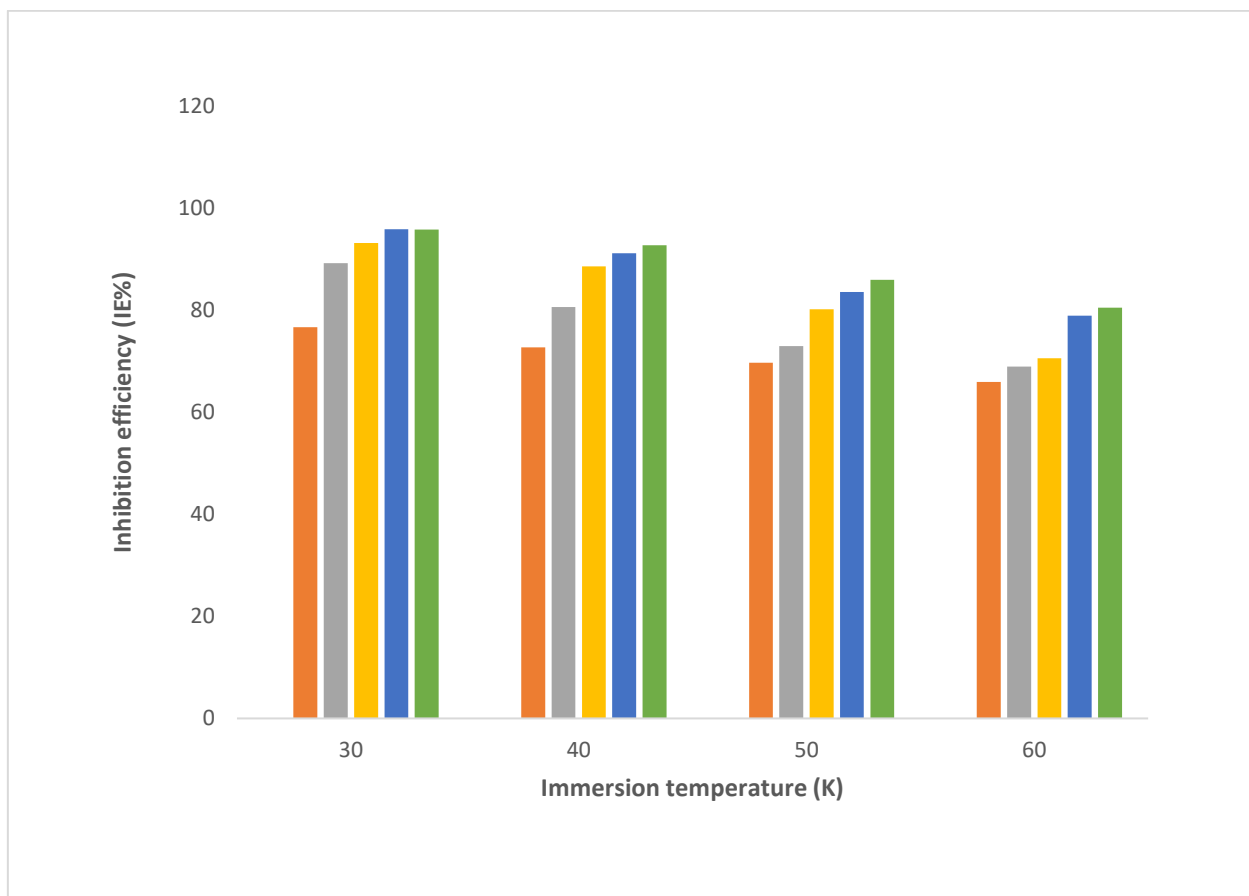


Fig. 5 – Variation of inhibition efficiency (% IE) with concentration of inhibitor at different temperatures (30–60°C).

Potentiodynamic polarization studies.

The Tafel plots of the corrosion behaviour of the samples are displayed in Figure 6 and Table 6 respectively. From the figure, it was observed that the average potential for the substrate shifted to a lower potential and higher current density. As the concentration of (*MC*) increases in the inhibiting, there was an increase in the corrosion potential of the inhibited samples. This increase in corrosion resistance obtained for the inhibited samples could be attributed to the various functional groups present in (*MC*). The polarization measurement results showed that the effect of the addition of *MC* extract on corrosion inhibition of steel pipelines in sulphuric acid decreased current density with an increase in inhibitor concentrations. The inhibition of both anodic and cathodic reactions was increased with an increase in *MC* extract concentrations.

Table 6 indicated that the effect of addition of *MC* extract on corrosion inhibition of mild steel in sulphuric acid decreased current density with increase in inhibitor concentration. The inhibition of both anodic and cathodic reactions were increased with an increase in *MC* extract concentration. Inhibitors indicated anodic or cathodic type when corrosion potential shifted more than 85 mV of the corrosion potential absence inhibitor. From the Table, E_{corr} shifted was less than 85 mV and can be classified as mixed type corrosion inhibitor^{1,4,8}. The Tafel plots show that the presence of the extract caused a decrease in both the anodic and cathodic current densities. The addition of *MC* extract to the H_2SO_4 solution reduces the anodic dissolution of iron and retards the cathodic hydrogen evolution reactions. Both corrosion current density and corrosion rate were considerably reduced in the presence of the extract.^{23,26}

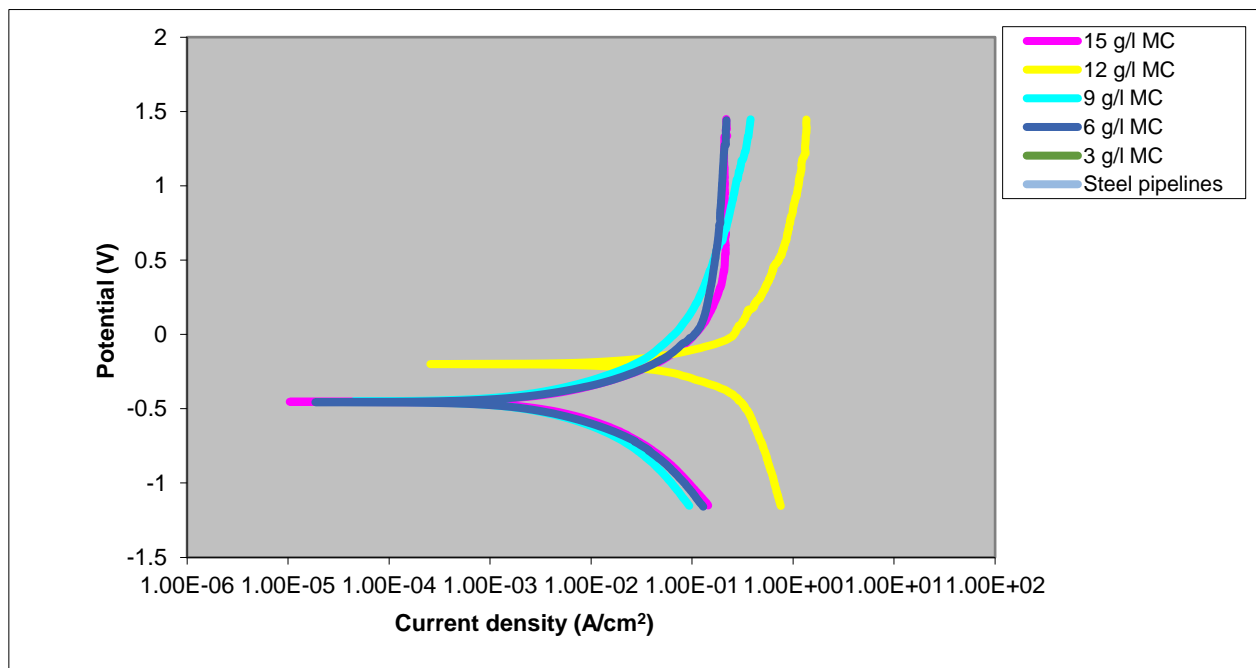


Fig. 6 – the Tafel curves for steel pipelines in 0.5 M H₂SO₄ in the absence and presence of MC extract concentrations at 30°C.

Table 6

The corrosion kinetic parameters of mild steel in 0.5 M H₂SO₄ in the absence and presence of MC extract at 30°C

MC(g/L)	-E _{corr} (SCE) (mV)	I _{corr} (mA/cm ²)	Tafel slopes (mV/decade)		Inhibition efficiency (IE %)
			b _a	b _c	
Control	0.502	8.691	72	90	–
3	0.549	0.779	73	93	91.02
6	0.550	0.610	74	94	93.00
9	0.521	0.539	75	95	93.80
12	0.547	0.478	76	95	94.50
15	0.546	0.479	76	96	94.48

Surface morphological analyses

The morphologies of the steel pipeline samples as received, without and with optimum concentrations in *Musanga cecropioides* (MC) in 0.5M sulphuric acid solutions were presented in Figs. 7, 8, and 9 respectively. Figure 7 presents the SEM morphology of steel pipelines of as-received samples in a polished state. Figure 8 is the polished sample in the presence of 0.5M H₂SO₄ solution without extract and Fig. 9 represents the polished sample in 0.5 M H₂SO₄ solution with the extract of MC at the optimum concentration of 12 g/l.

The surface of the coupon in Fig. 7 was completely smooth, without any indentations except

the polished surface that was revealed. In Fig. 8, the pits initiation commenced which is often linked to the presence of local defects at the metal surface such as flaws in the oxide or segregation of alloying elements, presence of aggressive anions such as sulphates in the environment. Pit initiation occurs on the alloy surface passivated by an oxide film due to the damage caused by passivation of the electrolyte resulting in an anodic reaction on the metal surface while the unexposed protective surrounding becomes the cathode leading to localized corrosion.³⁵ As time progresses, the growth of pits increases from the SEM evaluation and obviously, the corrosion resistance decreases which confirmed that both weight loss and Tafel

results obtained are in agreement with each other and similar to the findings.^{36,37} Figure 9 coupon exposed to corrodent in the presence of optimum concentration was less rough, and neat, and the quality of the steel pipelines was enhanced in the presence of the extract. Hence, the propagation of pits in the coupon was impeded by the adsorption of

the inhibitor on the steel pipeline's surface. The adsorption of components of *MC* leaf extract could be attributed to their functional groups obtained from phytoconstituents and FT-IR results. The *MC* can be considered to be a good and effective corrosion inhibitor of material in sulphuric acid and is similar to the previous findings.³⁸⁻⁴⁰

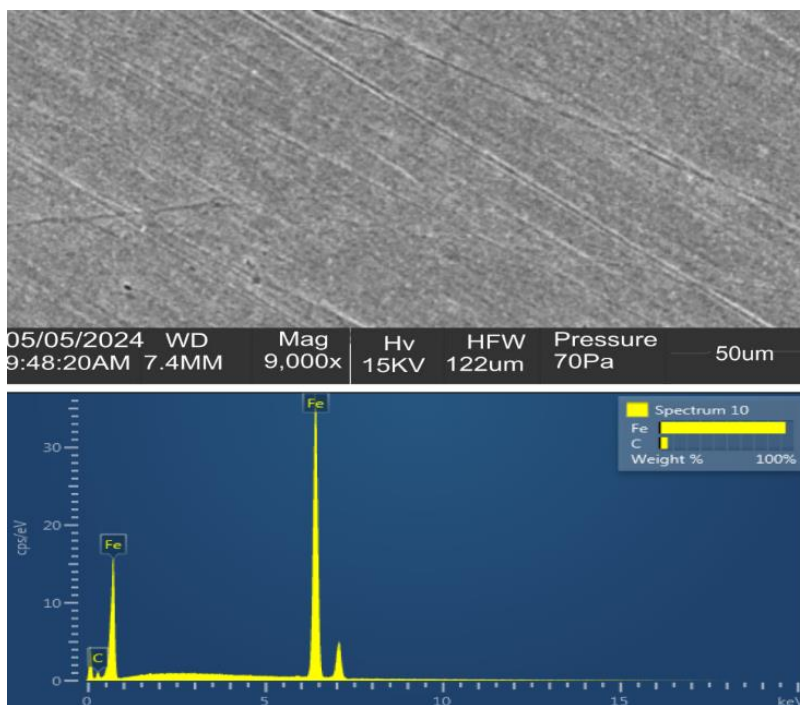


Fig. 7 – SEM/EDS of as-received steel pipelines coupon.

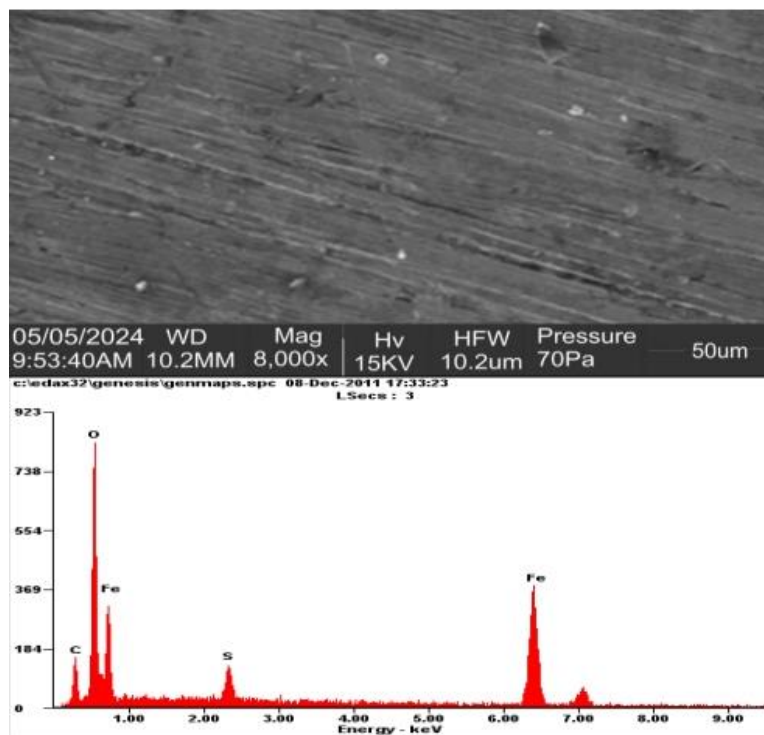


Fig. 8 – SEM/XRD of steel pipelines in 0.5 M H₂SO₄ in the absence of *MC* extract.

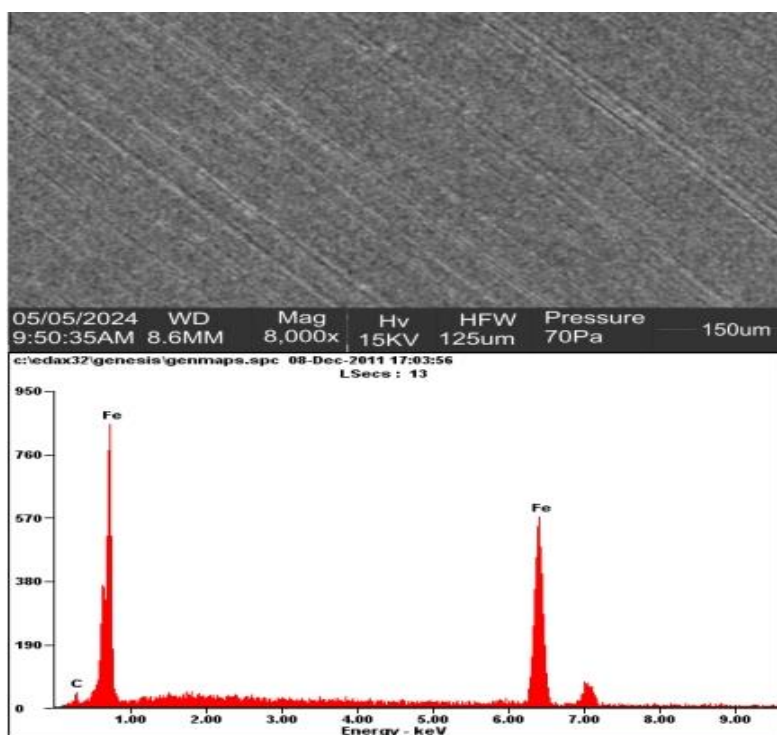


Fig. 9 – SEM/XRD of steel pipelines in the presence of an optimum inhibitor of *MC*.

CONCLUSIONS

From the research work carried out, the following conclusion can be drawn:

Musanga cecropioides (*MC*) leaf extracts represent a promising, eco-friendly, and cost-effective corrosion inhibitor for protecting oil and gas equipment in acidic environments, aligning with the industry's sustainable and efficient operations goals.

The gravimetric weight loss technique showed the inhibiting effect of *MC* with a percentage inhibition efficiency of 95.76% at 12 g/l but decreased with increasing temperature.

The extracts exhibit excellent corrosion inhibition properties in acidic environments, primarily attributed to the presence of bioactive compounds such as alkaloids, flavonoids, tannins, and saponins. These compounds adsorb onto metal surfaces, forming a protective barrier that minimizes corrosion.

The corrosion inhibition efficiency of *Musanga cecropioides* (*MC*) increases with the increase in the concentration of inhibitor to an optimum at 12 g/l, the inhibition efficiency was highest at 30°C and decreased with an increase in temperature from 30 to 60°C.

The FT-IR revealed some major constituents such as Chlorocompound, Aromatic phosphates, Amine, and Carboxyl acid which were adsorbed onto the steel pipeline surface in 0.5 M H₂SO₄ solution and the morphology of the adsorbed protective films on the steel pipeline surface confirmed the high performance of the inhibitor of *Musanga cecropioides* (*MC*).

Acknowledgement. The authors highly appreciate and acknowledge the Africa Centre of Excellence for Sustainable Power and Energy Development, ACE-SPED, University of Nigeria, Nsukka, Energy Materials Research Group, University of Nigeria, Nsukka, Nigeria, Department of Metallurgical and Materials Engineering, University of Nigeria and University of Ibadan, Nigeria.

REFERENCES

1. I.Y. Suleiman, K. Mu'azu, A. D. Omah Egoigwe V. S, R. E. Njoku, *Rev. Roum. Chim.*, **2024**, 69, 171–182. <https://doi.org/10.33224/rch.2024.69.3-4.07>
2. M. E. S. De Jesus, et al, *Braz. J. Dev.*, **2020**, 6, 77197–77215... <https://doi.org/10.34117/bjdv6n10-227>
3. M. Finšgar, and J. Jackson, *Corros Sci.*, **2014**, 86, 17-41. <https://doi.org/10.1016/j.corsci.2014.04.044>
4. I. Y. Suleiman and A. S Sani, *Iran. J. Sci. Technol. Trans. A Sci.*, **2018**, 42, 1977–1987. <https://doi.org/10.1007/s40995-017-0384-9>

5. I. Y. Suleiman, A. Kasim, M. Z. Sirajo, A. T. Mohammed, *Rev Roum Chim.*, **2020**, 65, 997-1007. <https://doi.org/10.33224/rch.2020.65.11.05>
6. I. Y. Suleiman et al., *Metall Mater Eng.*, **2017**, 23, 153–166.
7. D. R. Gusti, I. Lestari, F. Farid, P. T. Sirait, *J. Phys. Conf. Ser.*, **2019**, doi:10.1088/1742-6596/1282/1/012083
8. V. Vorobyova, M. E. Skiba, *S. Afr. J. Chem. Eng.*, **2023**, 43, 273–295 <https://doi.org/10.1016/j.sajce.2022.11.004>
9. O. Sotelo-Mazon, S. Valdez, J. Porcayo-Calderon et al., *Prot. Met. Phys. Chem. Surf.*, **2020**, 56, 427–437 <https://doi.org/10.1134/S2070205120020240>
10. A. Singh, V. K. Singh, M. A. Quraishi, *J. Mater. Environ. Sci.*, **2010**, 1: 162–174.
11. C. Bouyahia et al., *Mor. J. Chem.*, 10, 738-751; doi.org/10.48317/IMIST.PRSM/morjchem-v10i4.32146
12. A. M. Abd Elkader et al., *Saudi J. Biol. Sci.*, **2022**, 29, 1428–1433, <https://doi.org/10.1016/j.sjbs.2021.11.031>
13. C. Castro-López et al., *Molecules* **2019**, 24, 173. <https://doi.org/10.3390/molecules24010173>
14. H. Lgaz, R. Salghi, S. Jodeh and B. Hammouti, *J. Mol. Liq.*, **2017**, 225, 271–280.
15. A. M. Ayuba, M. A. Auta, N. U. Shehu, *Green appld Chem J*, **2021**, 13, 66–86; doi: 10.48419/IMIST.PRSM/rhazes-v13.28980
16. M. Yadav, L. Gope, N. Kumari, P. Yadav, *J. Mole. Liqs*, **2016**, 216, 78–86.
17. K. R. Ansari, M.A. Quraishi *J. Ind. Eng. Chem*, 2015 25, 89–98
18. T. David, T. James, “*CRC Series*, **1998**, 1-390.
19. A. S. Fouda, M. A. Ismail, G.Y. Elewady, A.S. Abousalem, *J. Mole. Liq*, **2017**, 240, 372–382.
20. M. Finšgar, J. Jackson, *Corr. Sci.*, **2014**, 86, 17–41.
21. O. Benali, C. Selles and R. Salghi, *Res. Chem. Intermediat.*, **2014**, 40, 259–268.
22. A. S. Fouda, M. A. Ismail, G. Y. Elewady and A. S. Abousalem, *J. Mol. Liq.*, **2017**, 240, 372–388.
23. A. H. Al-Moubaraki, A. Al-Judaibi, A. Maryam, *Int. J. Electrochem. Sci.*, **2015**, 10, 4252–4278
24. M. Yadav, K. Gope, N. Kumari and P. Yadav, *J. Mol. Liq.*, **2016**, 216, 78–86.
25. 5. K. R. Ansari, M. A. Quraishi and A. Singh, *J. Ind. Eng. Chem.*, **2015**, 25, 89–98.
26. M. Babutzka, A. Heyn, P. Rosemann, *Maters Corros.*, **2018**, 24, 1–12.
27. N. Chaubey, D. K. Yadav, V. K. Singh, M. Quraishi, *Ain Shams Eng. J.*, 2017, 8, 673–682.
28. R. T. Olorunmota et al., *J Adv Biol. Biotechnol.*, **2017**, 16, 1–9.
29. N. J. Salazar-López et al., *Food Res. Inter.* **2020**, 138, Part A 109774, <https://doi.org/10.1016/j.foodres.2020.109774>
30. K. A. Kenneth, M. A. Tolulope, A. O. Peter, *J Mater Res Technol.*, **2014**, 3, 9–16
31. H. Lgaz et al., *J Mol Liq.*, **2017**, 225, 271–280. <https://doi.org/10.1016/j.molliq.2016.11.039>
32. M. S. Al-Otaibi et al., *Arab J Chem.*, **2014**, 7, 340–346
33. M. Wang, P. Yu, A.G. Chittiboyina, D. Chen, J. Zhao, B. Avula, Y.-H. Wang, I.A. Khan, *Molecules (Basel, Switzerland)* **2020**, 25, 1453
34. N. J. Salazar-López, J. A. Domínguez-Avila, E. M. Yahia, B. H. Belmonte-Herrera, A. Wall-Medrano, Ef. Montalvo-González, G.A. González-Aguilar, *Food Res. Inter.* 138, Part A, **2020**, 109774
35. M. A. Tremocoldi, P. L. Rosalen, M. Franchin, A. P. Massarioli, C. Denny, É. Regina Daiuto, J. A. Rizzato Paschoal, P. Siqueira Melo, S. M. de Alencar, *Plos One*, **2018**, 13, <https://doi.org/10.1371/journal.pone.0192577>
36. C. Castro-López, I. Bautista-Hernández, M.D. González-Hernández, G.C.G. Martínez-Ávila, R. Rojas, A. Gutiérrez-Díez, N. Medina-Herrera, V.E. Aguirre-Arzola, *Molecules*, **2019**, 24, 17
37. J. C. da Rocha, J.A.C.P Gomes, *Materials (Rio de Janeiro)* (2017) 22(Suppl 1): e11927.
38. J. C. Rocha, J. C. Gomes, E. D'Elia, *Maters. Res*, 17, **2014**, 1581–1587.
39. Z. Zhang, N.C. Tian, X.D. Huang, W. Shang, L. Wu, *RSC Adv*, **2016**, 6, 22250–22268.
40. M.E.S. de Jesus, A. de Mendonça Santos, M.S. Tokumoto, F. Cotting, I.P. Aquino, V.R. Capelossi, *Brazilian J. Develo.*, **2020**, 6, 77197–77215